Global patterns and climatic controls of belowground net carbon fixation

Laureano A. Gherardi[a,b,1] and Osvaldo E. Sala[a,b,c]

[a]Global Drylands Center, Arizona State University, Tempe, AZ 85287-4501; [b]School of Life Sciences, Arizona State University, Tempe, AZ 85287-4501; and [c]School of Sustainability, Arizona State University, Tempe, AZ 85287-4501

Edited by William H. Schlesinger, Cary Institute of Ecosystem Studies, Millbrook, NY, and approved July 1, 2020 (received for review April 8, 2020)

Carbon allocated underground through belowground net primary production represents the main input to soil organic carbon. This is of significant importance, because soil organic carbon is the third-largest carbon stock after oceanic and geological pools. However, drivers and controls of belowground productivity and the fraction of total carbon fixation allocated belowground remain uncertain. Here we estimate global belowground net primary productivity as the difference between satellite-based total net primary productivity and field observations of aboveground net primary production and assess climatic controls among biomes. On average, belowground carbon productivity is estimated as 24.7 Pg y^{-1}, accounting for 46% of total terrestrial carbon fixation. Across biomes, belowground productivity increases with mean annual precipitation, although the rate of increase diminishes with increasing precipitation. The fraction of total net productivity allocated belowground exceeds 50% in a large fraction of terrestrial ecosystems and decreases from arid to humid ecosystems. This work adds to our understanding of the belowground carbon productivity response to climate change and provides a comprehensive global quantification of root/belowground productivity that will aid the budgeting and modeling of the global carbon cycle.

global C cycle | BNPP | primary production | allocation | root production

Terrestrial ecosystems annually offset approximately 20% of the carbon dioxide in anthropogenic emissions (1), providing a crucial ecosystem service under the Anthropocene. This carbon sequestration results from the excess of net primary production (NPP) over heterotrophic respiration (2). Plants allocate a significant fraction of total net primary production belowground, primarily to roots (3). Belowground net primary productivity (BNPP) strongly affects the global carbon cycle, as root growth (4) and rhizodeposition (5) are the main sources of soil organic carbon. Functionally, roots are the main belowground resource acquisition organs and play an important role in the uptake of water and nutrients supporting global productivity (6). In addition, belowground productivity is the energy source supporting soil microbial and faunal life and a vast assemblage of key ecological processes (7). Despite the significant importance of this carbon cycling pathway, however, some basic processes, such as climatic controls of global BNPP and primary productivity allocation patterns among biomes, remain underexplored, hindering our understanding of the mechanisms controlling the most uncertain component of the global carbon budget (8).

Current global carbon cycle modeling and budgeting efforts draw on a vast literature regarding patterns and controls of total and aboveground net primary productivity from local to global scales (2, 9–11). However, the carbon allocated belowground cycles at different rates and is governed by different drivers than aboveground carbon (12). Individual field studies have shown contrasting BNPP responses to environmental variables. In water-limited ecosystems, such as deserts, grasslands, shrublands, and savannas, BNPP increases with annual precipitation (13), with a mixed response to grazing (14). In forest ecosystems, BNPP is affected by belowground resources, such as nutrient availability and soil moisture, in temperate sites (15) and by light and temperature in tropical ecosystems (16). However, there is no unifying analysis exploring global BNPP patterns across biomes using a consistent methodology. The following questions remain unanswered: What is the global magnitude of BNPP? Does BNPP change with precipitation in a similar fashion as aboveground net productivity (ANPP)? Does the response of BNPP to climate vary among biomes?

Our present work addressed four objectives: (i) to estimate BNPP at global scale, (ii) to assess the relative importance of biome-specific BNPP in the global carbon cycle, (iii) to investigate the effect of climate and biome type on BNPP and the fraction of total net primary productivity allocated belowground (F-BNPP = BNPP/[BNPP + ANPP]); and (iv) to explore global geographical patterns of BNPP and F-BNPP. Here we present an approach to studying global patterns and controls of BNPP and F-BNPP that combines complementary data types.

Results and Discussion

Global BNPP Estimation. NPP is defined as the rate of plant organic matter accumulation exceeding plant respiratory efflux during a period of measurement (17). BNPP, the fraction of NPP occurring in the soil, is not quantifiable in a strict sense (18). Conceptually, BNPP equals the sum of the positive changes in belowground biomass, the amount of biomass consumed by herbivores, the amount of biomass lost to death, and the amount of rhizodeposits during a specific time interval (17). Given the difficulty in estimating all BNPP components (19, 20), most previous studies have focused on root production, defined as the increase in live root biomass plus root mortality per unit of time.

Significance

The fraction of fixed carbon allocated belowground in terrestrial ecosystems is the most uncertain component of global carbon cycle assessments. Here we present a novel approach to determining global quantification of belowground productivity, which is estimated at 24.7 Pg y^{-1} and accounts for 46% of terrestrial carbon fixation. Carbon allocated belowground has a longer residence than its aboveground counterpart, playing a key role in long-term carbon storage. Total belowground productivity increases with precipitation, but the rate of increase decreases from arid to humid ecosystems. The fraction of total fixed carbon entering the soil decreases with precipitation and varies significantly among biomes. These results are indicative of the possible impacts of climate and land use changes on the global carbon cycle.

Author contributions: L.A.G. and O.E.S. conceived the idea for the project; L.A.G. collected, compiled, and analyzed the data; and L.A.G. and O.E.S. wrote the paper.

The authors declare no competing interest.

This article is a PNAS Direct Submission.

Published under the PNAS license.

[1]To whom correspondence may be addressed. Email: Lau@ASU.edu.

This article contains supporting information online at https://www.pnas.org/lookup/suppl/doi:10.1073/pnas.2006715117/-/DCSupplemental.

First published August 3, 2020.

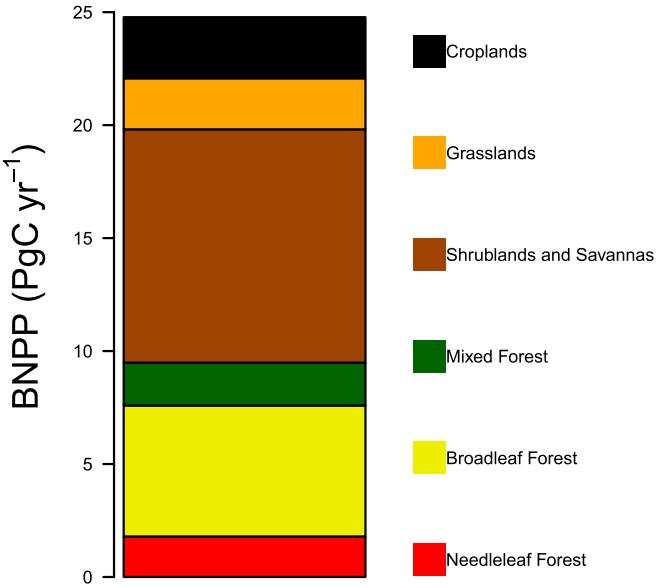

Fig. 1. Global BNPP and its partitioning among biomes. Total Global BNPP was 24.7 ± 5.7 Pg C y^{-1} BNPP was estimated using the best model according to AIC scores relating BNPP and MAP (*SI Appendix*, Table S1). CIs for each biome are presented in Table 1.

Recent studies have highlighted the importance of rhizodeposits as a major input to soil carbon formation (5). Here we estimated BNPP as the difference between satellite-derived total NPP and mean ANPP from field observations at 111 sites (*SI Appendix*, Fig. S1):

$$\text{Estimated BNPP}_{\text{site}} = \text{satellite NPP}_{\text{site}} - \text{field ANPP}_{\text{site}}. \quad [1]$$

The derivation of NPP from satellite information follows original ideas outlined by Monteith (21) suggesting that NPP is related to the amount of solar energy absorbed by plants. Satellite measurements of absorbed photosynthetically active radiation multiplied by energy conversion efficiency result in widely used estimates of total NPP (22), the sum of what is allocated aboveground and belowground. The energy conversion coefficient plays a key role in the estimation of NPP. The current version of the US National Aeronautics and Space Administration (NASA) NPP product uses a potential energy conversion efficiency obtained from wheat crop values, and the Biome BGC model sets climatic and biogeochemical constraints (23). This way, each location at each time point has a specific conversion efficiency that considers precipitation, temperature, and nutrient availability, among other variables. However, such efficiency pertains to total NPP and does not allow for estimation of individual components of productivity either aboveground or belowground.

Ecologists use various approaches to measure ANPP and BNPP in the field. The most common include harvesting of biomass aboveground or ingrowth cores belowground and estimating productivity as the increase in biomass through time (19, 24). We combined field and satellite approaches to estimate BNPP (Eq. **1**) and validated our BNPP estimates against direct field root productivity (RP) measurements (*SI Appendix*, Fig. S2). We used 15-y mean NPP derived from satellite data and the mean ANPP from field measurements for the longest record possible in 111 sites around the world (*SI Appendix*, Table S5). Long-term satellite NPP and field ANPP data capture major global patterns incorporating year-to-year variations in productivity. Similarly, we only included sites that measured productivity in multiple plots or locations within a site, to include spatial variability and obtain a representative estimate of local productivity. We took this conservative approach to minimize errors due to different scales of field and satellite observations.

Estimated BNPP was closely related to RP field observations across 40 sites (slope = 0.83, $P = 0.0001$, $R^2 = 0.61$, $n = 40$) (*SI Appendix*, Fig. S2). This relationship is notable, given that field data were collected using different methods and came from diverse ecosystems that varied with respect to climate, species composition, and soil type. The slope of the model is not significantly different from 1 (95% CI = 0.61 to 1.05), whereas the intercept is significantly different from 0 (intercept = 225.1, $P = 0.0001$), highlighting the importance of other components of BNPP beyond RP across biomes (25). The relatively strong correlation between field RP and estimated BNPP may be the result of greater differences among sites compared with differences among time periods and methods.

Global BNPP and F-BNPP and Their Controls. Long-term mean global BNPP totaled 24.7 ± 5.7 Pg C y^{-1} (Fig. 1 and Table 1). This value indicates that at the global scale, BNPP is ∼46% of total terrestrial NPP. This global value is smaller than most previous estimates based on individual sites, in which grassland F-BNPP ranged from 50% to 66% (26), forest ecosystem F-BNPP ranged from 20% to 65% (27), and shrubland F-BNPP ranged from 58% to 78% (28). We suggest that these previous estimates could have been driven by a focus on short-stature ecosystems, which tend to have a larger F-BNPP than forest ecosystems. The contributions of the different biomes to global BNPP depend on their mean BNPP per unit area and the areal extent. Shrublands and savannas contribute the most to global BNPP because of their large cover and relatively large F-BNPP. The next greatest contributor is broadleaf forests, which have a higher BNPP per unit area but a smaller areal extent (Table 1).

BNPP increased nonlinearly from arid to humid sites, showing a decreasing rate of increase with precipitation (Fig. 2). The nonlinear nature of the relationship between BNPP and mean annual precipitation (MAP) provides evidence of a strong water limitation of BNPP in arid ecosystems that decreases as the MAP increases to a point at which BNPP is probably limited by resources other than water. We suggest that the BNPP:MAP slope is associated with the frequency at which water availability limits primary productivity, which declines as MAP increases and other factors start to contribute more strongly (29). The shape of the

Table 1. Global and biome-scale belowground productivity

Parameter	Needleleaf forest	Broadleaf forest	Mixed forest	Shrublands and savannas	Grasslands	Croplands	Global
BNPP, Pg C y^{-1}	1.8 ± 0.38	5.8 ± 0.89	1.9 ± 0.33	10.3 ± 2.4	2.3 ± 0.62	2.7 ± 0.81	24.7 ± 5.7
Mean F-BNPP, %	58 ± 4.3	41 ± 4.8	54 ± 3.9	61 ± 4.8	64 ± 5	32 ± 4	46 ± 7.4
Mean BNPP, g m^{-2} y^{-1}	227 ± 49	336 ± 52	251 ± 46	210 ± 53	194 ± 55	152 ± 47	220 ± 76
Biome area, millions of km^2	7.6	17.1	7.3	45.3	11.1	17.5	106

Shown are total BNPP, mean F-BNPP, mean BNPP per unit area, and areal extent for six biomes and the total for terrestrial ecosystems. Values represent total or mean ± 2 SE. BNPP was estimated using a global model relating BNPP and MAP (Fig. 2) for each pixel and summing all pixels for each biome. F-BNPP was estimated using a global model relating F-BNPP and MAP (Fig. 3) for each pixel and calculating the average of all pixels for each biome.

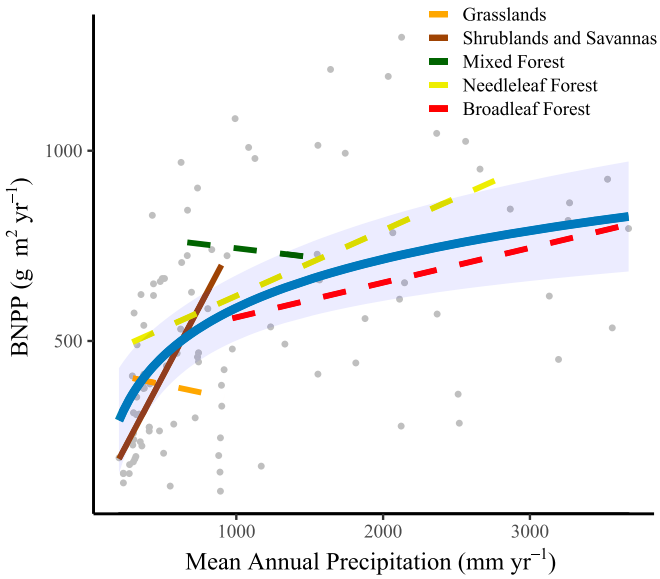

Fig. 2. At the global scale, BNPP increases with MAP, but the rate of increase decreases with precipitation. Individual biomes have idiosyncratic responses of belowground production to precipitation increasing or decreasing with MAP (BNPP at the global scale = −688 + 184 * log (MAP), $P_{\text{logarithmic term}} < 0.001$, ΔAIC = 4.45, $R^2_{\text{conditional}} = 0.36$). These models represent the best fit among linear and nonlinear models compared using the AIC. Colored lines indicate linear trends for each biome. The shaded blue region around the blue line represents the 95% CI.

BNPP:MAP relationship is similar to that of ANPP (*SI Appendix*, Fig. S4) (30) and total productivity (*SI Appendix*, Fig. S3).

Within biomes, only shrublands and savannas showed a significant BNPP increase with MAP, whereas all other biomes showed a nonsignificant relationship to precipitation (*SI Appendix*, Table S3). The lack of response of BNPP to MAP is surprising for the grassland biome, which typically shows a strong positive relationship between ANPP and precipitation (31). We suggest that the lack of response of grassland BNPP to MAP can be explained by the sharp decline in F-BNPP with MAP, which offsets the effects of increasing NPP. In contrast, forest BNPP is likely controlled by nutrient availability (32) or incoming solar radiation (33), explaining the flattening of the curve at high MAP.

Globally, MAP is the climatic variable accounting for most of the spatial variation in BNPP. We fitted 20 different mixed models, including linear and nonlinear combinations of BNPP, as a function of ten bioclimatic variables (34). We also included a model considering a precipitation by temperature interaction based on previous findings in forest ecosystems (35). A logarithmic model of BNPP as a function of MAP resulted in the lowest AIC score (*SI Appendix*, Table S1). The other nine climatic variables included precipitation and temperature for the wettest, driest, warmest, and coldest quarter of the year.

The F-BNPP has multiple implications for ecosystem functioning (36, 37). The functional balance theory states that plants may adjust biomass allocation in a way that minimizes resource limitation (38). Allocation aboveground generally promotes leaf area, transpiration, and photosynthesis, whereas allocation belowground stimulates the acquisition of water and nutrients (39). The fraction of total carbon fixation allocated belowground has further implications for carbon sequestration in terrestrial ecosystems (40), because belowground carbon has a much longer residence time than aboveground carbon (41) due to a slower decomposition rate (42). Climatic and environmental conditions influence F-BNPP in diverse ways (43, 44). It is generally accepted that plants allocate relatively larger fractions of productivity belowground under increasing drought conditions (20) or when limited by soil nutrient availability (45, 46). Enhanced carbon dioxide concentration in the atmosphere can have direct impacts on allocation (27) or affect F-BNPP through changes in nitrogen limitation (39). The specific plant species composition across biomes also constrains the allocation of primary production in different ecosystems (3).

F-BNPP was found to decrease logarithmically with increasing MAP at the global scale (Fig. 3 and *SI Appendix*, Table S2), ranging from ∼70% in arid ecosystems to ∼35% in humid ecosystems. Values of F-BNPP and the relationship between F-BNPP and MAP (*SI Appendix*, Fig. S5) agree with a synthesis of previous data (44, 47), providing independent support for the results obtained using a combination of field data and remote sensing data. Ecosystem carbon allocation reflects plant allocation to roots vs. aboveground organs such as leaves, branches, and twigs (37). Plant species that evolved in arid ecosystems may have a competitive advantage, with allocation patterns that destine more resources for belowground, enhancing their capacity for acquiring water while minimizing water loss through transpiration. In contrast, plant species that evolved in more mesic environments, such as forest ecosystems, may exhibit the opposite allocation pattern (32, 43). Water-limited ecosystems such as deserts, grasslands, and shrublands allocate a larger fraction of fixed carbon belowground (Table 1). There is evidence of a strong water limitation of primary production in drylands that gradually switches to nitrogen limitation (29) and then to multiple nutrient limitation (48) as MAP increases. Forest ecosystems transition from colimitation by belowground and aboveground resources due to temperature-limited nutrient mineralization in boreal and temperate forests (49) to limitation by aboveground resources in tropical ecosystems (32). Along a latitudinal gradient, symbiotic associations typical at high-latitude forests are replaced by adaptations to fast biogeochemical cycling at low latitudes (32). Therefore, tropical forests show the smallest fraction of NPP allocated belowground among unmanaged ecosystems. Finally, croplands allocate the smallest

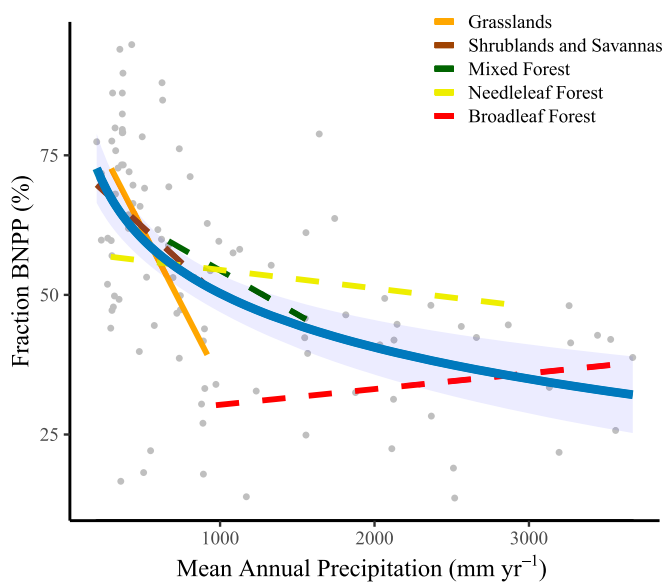

Fig. 3. At the global scale, the F-BNPP declined exponentially with MAP. Biomes showed idiosyncratic linear responses to MAP, with slopes ranging from negative to positive F-BNPP as a function of MAP (F-BNPP = 146 − 13.95 * log (MAP), $P_{\text{logarithmic term}} < 0.0001$, ΔAIC = 10.25, $R^2_{\text{conditional}} = 0.32$). These models represent the best fit among linear and nonlinear models compared using the AIC. Colored lines indicate trends for each biome. The shaded blue region around the blue line represents the 95% CI.

fraction of productivity to belowground organs, likely due to the historical breeding aimed at increasing allocation to harvestable products and to growth under fertilization and irrigation conditions.

This study addresses the climatic controls of BNPP and F-BNPP and also suggests a potential effect of land use change. Phenomena such as agricultural expansion may result in biome shifts that lead to changes in BNPP and F-BNPP. Even though croplands maintain relatively high total productivity, the small fraction of productivity allocated belowground by crops results in low BNPP for this biome. Agricultural expansion may lead to net soil carbon release due to drastic changes in productivity allocation in addition to the enhanced decomposition resulting from tillage (42).

Conclusion

Geographic patterns of BNPP reflect those of total productivity (Fig. 4*A*), with high productivity in tropical ecosystems decreasing toward arid ecosystems. Patterns of F-BNPP are opposite of those of BNPP, with relatively larger belowground allocation in arid ecosystems compared with mesic ecosystems (Fig. 4*B*). In synthesis, the contribution of biome to global BNPP is associated with NPP but is modulated by allocation patterns. Spatial patterns of BNPP and their correlation with precipitation gradients provide hints about the consequences of climate change. However, ecologists have long recognized the differences between controls of productivity in space and in time (50). Differences in productivity among locations with different MAP levels are much larger than changes in productivity due to intrasite precipitation variation of similar magnitude occurring from year to year. The paucity of long-term BNPP and F-BNPP data, particularly in forest ecosystems, constrained our ability to assess patterns over time. Further investigations of BNPP and F-BNPP responses to changes in precipitation over time are needed to accurately estimate the effects of the expected changes in precipitation amount and frequency of extreme events on the fate of carbon fluxes and stocks. Experimental field studies of BNPP and F-BNPP in which precipitation and nutrients are manipulated while other drivers are kept constant would be particularly useful for identifying cause-and-effect relationships. These studies would complement the more abundant observational studies included in this work. Finally, the insights gained here are relevant to the understanding and modeling of the carbon cycle, given that BNPP remains the least constrained component of the global carbon budget (8).

Materials and Methods

To address our study objectives, we combined data from complementary sources, including field ANPP, field RP, and satellite-derived NPP data, to estimate BNPP. We also used interpolated climate data as a consistent source of climatic variables across sites (34).

Data Collection.

Field ANPP and RP. We collected field ANPP data for the longest record possible from 111 locations around the world covering all major biomes (*SI Appendix*, Fig. S1). Our database spans forest cover types including broadleaf, needle leaf, evergreen, deciduous, and mixed forest; open and closed shrublands; savannas and woody savannas; croplands; and grasslands ranging from desert steppes to prairies. We collected ANPP estimates that included fine and coarse components (ANPP = ANPP_foliage + ANPP_woody) and included only sites that reported multiple years and multiple plots. Including multiple years and multiple plots provided a broad estimation of the productivity that integrates year-to-year variation and intrasite spatial heterogeneity.

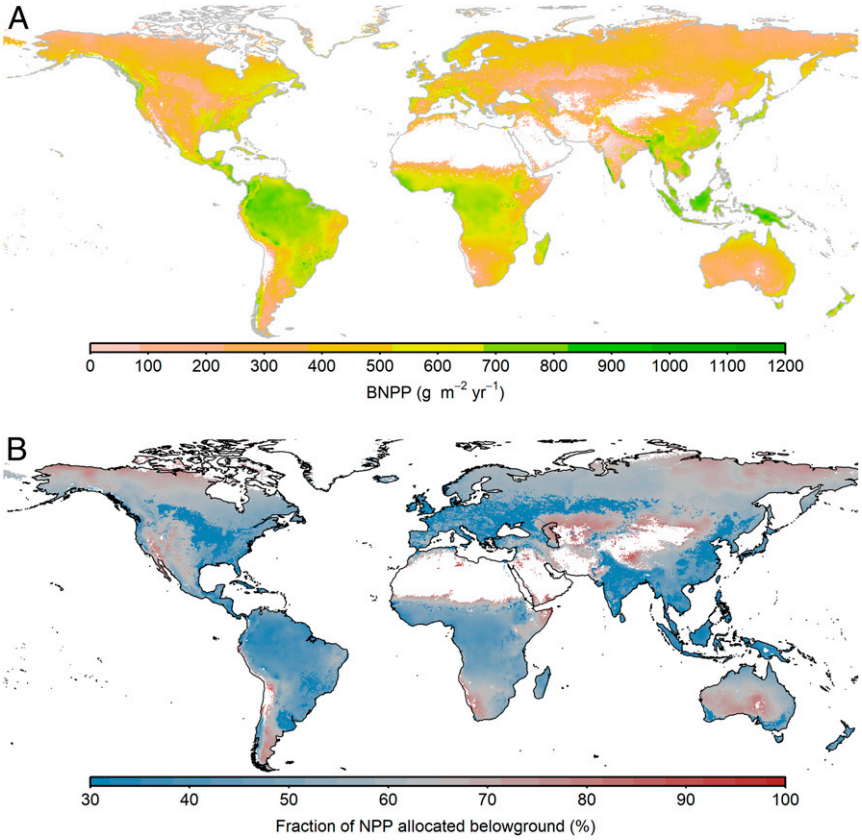

Fig. 4. Geographical patterns of BNPP and the fraction of productivity allocated belowground. (*A*) Global BNPP geographical patterns across major biomes. (*B*) Global F-BNPP patterns across major biomes. BNPP and F-BNPP were estimated using the best-fitting model after testing combinations of 10 climatic variables and precipitation by temperature interactions (*SI Appendix*, Tables S1 and S2).

Therefore, our criteria for using multiple years and plots reflect our approach to matching the scales of field and remotely sensed data, which have a resolution of 1 km^2 and an average of multiple years. Data limitations forced us to group land cover types into six biome categories. We combined deciduous and evergreen forests within each forest category as needleleaf, broadleaf, and mixed forests. We also grouped open shrublands, closed shrublands, savannas and woody savannas as one category for shrublands and savannas. Grasslands and croplands represent the original cover type classification. We collected data from existing databases, including the Long-Term Ecological Research network, the EcoTrends project, the Oak Ridge National Laboratory (ORNL) net primary production database, and the ForC database (51) (*SI Appendix*, Table S5). We also used data from publications or directly from researchers whenever it was not available through a data repository. In addition, we collected field RP data (RP = P_fine roots + P_coarse roots) from the ORNL and ForC databases and from publications for 40 sites to validate our estimated BNPP.

Satellite-derived productivity data. We extracted total NPP data available from the NASA Earth Observing System, which produces annual estimates of net primary productivity (NPP) of the entire terrestrial earth surface at 1-km spatial resolution derived from the Moderate-Resolution Imaging Spectroradiometer (MODIS). The derivation of NPP has three components: (i) the assumption that NPP is related to the amount of solar energy absorbed by the Earth's surface; (ii) the theory relating absorbed solar energy and spectral indices of vegetation; and (iii) the assumption that the actual energy conversion efficiency is limited by climatic and biophysical constraints to below the theoretical potential value. A more detailed description of the algorithm and product derivation can be found in the user guide (www.ntsg.umt.edu/files/modis/MOD17UsersGuide2015_v3.pdf) and other reports (22, 52). Despite some recent criticism, we argue that this NPP product is reliable at the broad scales used in this study. Finally, the MODIS NPP shows agreement with modeled and in situ observations of productivity (53).

To have a consistent land cover classification source for all sites, we extracted land cover classes for each site from the MODIS land cover product MOD12Q1 based on Boston University's UMD classification scheme (54).

Interpolated climate data. We obtained data for 10 bioclimatic variables from Worldclim version 2 (34). The bioclimatic variables included MAP, mean annual temperature, and mean temperature and precipitation for different quarters of the year, such as the wettest quarter, driest quarter, warmest quarter, and coldest quarter. This database consists of monthly interpolated data from thousands of weather stations across 23 regions of varying size classified based on station density. This database is widely used, reliable, and consistent across sites.

BNPP Estimation. We estimated BNPP by subtracting ANPP from total NPP [**1**]:

$$EstimatedBNPP_s = NPP_s - ANPP_s,$$

where $BNPP_s$ is the estimated mean BNPP at site *s*, NPP_s is the 15-y mean NPP at site *s*, and $ANPP_s$ is the mean ANPP at site *s* for all available years. The estimated BNPP correlated with field measurements of RP across 40 sites at which the slope of the field RP vs. the estimated BNPP did not differ significantly from 1 (*SI Appendix*, Fig. S2). However, the intercept of such relationships did differ significantly from 0, suggesting that RP underestimates BNPP. We estimated cropland BNPP by multiplying total NPP by the mean of known root:shoot ratios estimated for the most common crops (55). Such root:shoot values match independent estimations specific for the cropland biome (47). Since crops rotate in unpredictable manner over time and vary across countries, we assumed that the mean root:shoot ratio for annual crops is a realistic coefficient for estimating mean long-term NPP partitioning.

In addition, we calculated the F-BNPP as the ratio of BNPP to total NPP for each site and expressed it as a percentage.

Data Analysis. We used simple linear regression to assess the relationship between RP from field measurements and estimated BNPP (*SI Appendix*, Fig. S2). We then ran linear and nonlinear mixed-model analyses of mean-estimated BNPP and F-BNPP as a function of each of the 10 bioclimatic variables. We included bioclimatic variables as fixed effects and biome as a random effect. We selected the best model using the Akaike information criterion (AIC) (56). Of all models including combinations of precipitation and temperature explanatory variables, a logarithmic model with MAP as an explanatory variable for BNPP had the lowest AIC value (*SI Appendix*, Table S1). All analyses, figure preparation, and data processing were carried out using R version 3.5.2 (57).

Global Belowground Productivity Estimation. To estimate global belowground productivity, we used the best model out of 25 models selected using the AIC (*SI Appendix*, Table S1) and related BNPP to all climatic variable combinations including linear and nonlinear alternatives. A nonlinear model including MAP as a single predictor resulted the best model for estimating BNPP at the global scale. We then estimated belowground productivity for each pixel using the Worldclim MAP product (Fig. 4*A*). Finally, we summed the BNPP of each pixel for each biome to estimate the total BNPP per biome (Fig. 1). In addition, we estimated the mean F-BNPP using the best model (Fig. 4*B*) and calculated mean biome F-BNPP as the mean of all pixels for each biome (Fig. 1). For croplands, we used a fixed mean allocation ratio of 0.32 from the literature (55) as the mean global F-BNPP and estimated BNPP by multiplying the NPP by this coefficient.

Global Belowground Productivity Uncertainty Estimation. To assess the uncertainty around our BNPP estimate, we calculated 95% confidence intervals (CIs) for the mixed-model fit of mean BNPP as a function of MAP (Figs. 2 and 3). This measure of uncertainty corresponds to the model, not to individual points, meaning that there is a 95% chance that the model-fit line will fall within that range. These bands result from doubling the SE from the generalized mixed model that considers fixed-effect error as well as the random effects of different biomes. Error terms vary with the magnitude of the independent variable, increasing as it deviates from the mean. Therefore, we extracted MAP-specific SEs from the output of the *lme* function in the *nlme* package (58) and doubled them to estimate the CI limits of BNPP for each grid cell using the *raster* package in R. Finally, we calculated the mean SE and derived CI limits for each biome and globally, presented in Table 1.

Data Availability. All data used in this work are freely available from the sources cited in the *SI Appendix*, Table S5. All code is available from the corresponding author on reasonable request.

ACKNOWLEDGMENTS. We acknowledge the work of all researchers that collected these data over the years. We appreciate the crucial contributions of organizations that gather, clean, and make data available, such as Oak Ridge National Lab, Ecotrends and the Long-Term Ecological Research Network. The comments and contributions of three anonymous reviewers and the journal editor improved this manuscript significantly. We thank Diana Wall, André C. Franco, and R.C. de Avellaneda for earlier discussion of ideas and input. This research was supported by Arizona State University, the Global Drylands Center, and the NSF (Grants DEB 14-56597, 17-54106, and 18-32194).

1. A. Arneth *et al*., Historical carbon dioxide emissions caused by land-use changes are possibly larger than assumed. *Nat. Geosci.* **10**, 79–84 (2017).
2. W. R. Wieder, C. C. Cleveland, W. K. Smith, K. Todd-Brown, Future productivity and carbon storage limited by terrestrial nutrient availability. *Nat. Geosci.* **8**, 441–444 (2015).
3. R. B. Jackson, H. A. Mooney, E.-D. Schulze, A global budget for fine root biomass, surface area, and nutrient contents. *Proc. Natl. Acad. Sci. U.S.A.* **94**, 7362–7366 (1997).
4. M. W. I. Schmidt *et al*., Persistence of soil organic matter as an ecosystem property. *Nature* **478**, 49–56 (2011).
5. N. W. Sokol, S. E. Kuebbing, E. Karlsen-Ayala, M. A. Bradford, Evidence for the primacy of living root inputs, not root or shoot litter, in forming soil organic carbon. *New Phytol.* **221**, 233–246 (2019).
6. J. K. Green *et al*., Large influence of soil moisture on long-term terrestrial carbon uptake. *Nature* **565**, 476–479 (2019).
7. D. H. Wall, Ed. *et al*., *Soil Ecology and Ecosystem Services*, (Oxford University Press, Oxford, United Kingdom, 2013).
8. C. Le Quéré *et al*., Global carbon budget 2017. *Earth Syst. Sci. Data* **10**, 405–448 (2018).
9. L. A. Gherardi, O. E. Sala, Effect of interannual precipitation variability on dryland productivity: A global synthesis. *Glob. Change Biol.* **25**, 269–276 (2019).
10. A. K. Knapp, M. D. Smith, Variation among biomes in temporal dynamics of aboveground primary production. *Science* **291**, 481–484 (2001).
11. H. L. Gholz, Environmental limits on aboveground net primary production, leaf area, and biomass in vegetation zones of the Pacific Northwest. *Ecology* **63**, 469–481 (1982).
12. J. Fortier, B. Truax, D. Gagnon, F. Lambert, Abiotic and biotic factors controlling fine root biomass, carbon and nutrients in closed-canopy hybrid poplar stands on post-agricultural land. *Sci. Rep.* **9**, 6296 (2019).
13. K. R. Wilcox *et al*., Asymmetric responses of primary productivity to precipitation extremes: A synthesis of grassland precipitation manipulation experiments. *Glob. Change Biol.* **23**, 4376–4385 (2017).
14. S. J. McNaughton, F. F. Banyikwa, M. M. McNaughton, Root biomass and productivity in a grazing ecosystem: The Serengeti. *Ecology* **79**, 587–592 (1998).
15. G. S. Newman, M. A. Arthur, R. N. Muller, Above- and belowground net primary production in a temperate mixed deciduous forest. *Ecosystems* **9**, 317–329 (2006).

16. C. M. Litton, C. P. Giardina, Below-ground carbon flux and partitioning: Global patterns and response to temperature. *Funct. Ecol.* **22**, 941–954 (2008).
17. E. P. Odum, G. W. Barrett, *Fundamentals of Ecology*, (W. B. Saunders, 1971), vol. 3.
18. W. K. Lauenroth, "Methods of estimating belowground net primary production" in *Methods in Ecosystem Science*, O. E. Sala, R. B. Jackson, H. A. Mooney, R. Howarth, Eds. (Springer, 2000), pp. 58–71.
19. D. A. Clark *et al*., Measuring net primary production in forests: Concepts and field methods. *Ecol. Appl.* **11**, 356–370 (2001).
20. D. G. Milchunas, W. K. Lauenroth, Belowground primary production by carbon isotope decay and long-term root biomass dynamics. *Ecosystems* **4**, 139–150 (2001).
21. J. L. Monteith, Solar radiation and productivity in tropical ecosystems. *J. Appl. Ecol.* **9**, 747–766 (1972).
22. S. W. Running *et al*., A continuous satellite-derived measure of global terrestrial primary production. *Bioscience* **54**, 547–560 (2004).
23. M. A. White, P. E. Thornton, S. W. Running, R. R. Nemani, Parameterization and sensitivity analysis of the BIOME–BGC terrestrial ecosystem model: Net primary production controls. *Earth Interact.* **4**, 1–85 (2000).
24. O. E. Sala, A. T. Austin, "Methods of estimating aboveground net primary production" in *Methods in Ecosystem Science*, O. E. Sala, R. B. Jackson, H. A. Mooney, R. W. Howarth, Eds. (Springer, 2000), pp. 31–43.
25. C. Martinez *et al*., Belowground carbon allocation patterns as determined by the ingrowth soil core 13C technique across different ecosystem types. *Geoderma* **263**, 140–150 (2016).
26. Y. Z. Gao *et al*., Belowground net primary productivity and biomass allocation of a grassland in Inner Mongolia is affected by grazing intensity. *Plant Soil* **307**, 41–50 (2008).
27. R. B. Jackson, C. W. Cook, J. S. Pippen, S. M. Palmer, Increased belowground biomass and soil CO_2 fluxes after a decade of carbon dioxide enrichment in a warm-temperate forest. *Ecology* **90**, 3352–3366 (2009).
28. A. Gorissen *et al*., Climate change affects carbon allocation to the soil in shrublands. *Ecosystems* **7**, 650–661 (2004).
29. L. Yahdjian, L. Gherardi, O. E. Sala, Nitrogen limitation in arid-subhumid ecosystems: A meta-analysis of fertilization studies. *J. Arid Environ.* **75**, 675–680 (2011).
30. T. E. Huxman *et al*., Convergence across biomes to a common rain-use efficiency. *Nature* **429**, 651–654 (2004).
31. O. E. Sala, L. A. Gherardi, L. Reichmann, E. Jobbágy, D. Peters, Legacies of precipitation fluctuations on primary production: Theory and data synthesis. *Philos. Trans. R. Soc. Lond. B Biol. Sci.* **367**, 3135–3144 (2012).
32. A. L. Gill, A. C. Finzi, Belowground carbon flux links biogeochemical cycles and resource-use efficiency at the global scale. *Ecol. Lett.* **19**, 1419–1428 (2016).
33. R. R. Nemani *et al*., Climate-driven increases in global terrestrial net primary production from 1982 to 1999. *Science* **300**, 1560–1563 (2003).
34. S. E. Fick, R. J. Hijmans, WorldClim 2: New 1-km spatial resolution climate surfaces for global land areas. *Int. J. Climatol.* **37**, 4302–4315 (2017).
35. S. Luyssaert *et al*., CO_2 balance of boreal, temperate, and tropical forests derived from a global database. *Glob. Change Biol.* **13**, 2509–2537 (2007).
36. R. B. Jackson *et al*., A global analysis of root distributions for terrestrial biomes. *Oecologia* **108**, 389–411 (1996).
37. P. B. Reich, "Root-shoot relations: Optimality in acclimation and adaptation or the 'emperor, s new clothes" in *Plant Roots: The Hidden Half*, Y. Waisel, A. Eshel, T. Beeckman, U. Kafkafi, Eds. (Marcel Dekker, 2002), pp. 205–220.
38. A. J. Bloom, F. S. Chapin, H. A. Mooney, Resource limitation in plants: An economic analogy. *Annu. Rev. Ecol. Syst.* **16**, 363–392 (1985).
39. H. Poorter *et al*., Biomass allocation to leaves, stems and roots: Meta-analyses of interspecific variation and environmental control. *New Phytol.* **193**, 30–50 (2012).
40. G. Chen, Y. Yang, D. Robinson, Allocation of gross primary production in forest ecosystems: Allometric constraints and environmental responses. *New Phytol.* **200**, 1176–1186 (2013).
41. J. B. Gaudinski, S. E. Trumbore, E. A. Davidson, S. Zheng, Soil carbon cycling in a temperate forest: Radiocarbon-based estimates of residence times, sequestration rates and partitioning of fluxes. *Biogeochemistry* **51**, 33–69 (2000).
42. S. Fontaine *et al*., Stability of organic carbon in deep soil layers controlled by fresh carbon supply. *Nature* **450**, 277–280 (2007).
43. R. E. McMurtrie, R. C. Dewar, New insights into carbon allocation by trees from the hypothesis that annual wood production is maximized. *New Phytol.* **199**, 981–990 (2013).
44. D. Hui, R. B. Jackson, Geographical and interannual variability in biomass partitioning in grassland ecosystems: A synthesis of field data. *New Phytol.* **169**, 85–93 (2006).
45. M. R. Keyes, C. C. Grier, Above- and below-ground net production in 40-year-old Douglas fir stands on low and high productivity sites. *Can. J. For. Res.* **11**, 599–605 (1981).
46. S. Vicca *et al*., Fertile forests produce biomass more efficiently. *Ecol. Lett.* **15**, 520–526 (2012).
47. S. T. Gower, C. J. Kucharik, J. M. Norman, Direct and indirect estimation of leaf area index, fAPAR, and net primary production of terrestrial ecosystems. *Remote Sens. Environ.* **70**, 29–51 (1999).
48. P. A. Fay *et al*., Grassland productivity limited by multiple nutrients. *Nat. Plants* **1**, 15080 (2015).
49. D. W. Kicklighter, J. M. Melillo, E. Monier, A. P. Sokolov, Q. Zhuang, Future nitrogen availability and its effect on carbon sequestration in northern Eurasia. *Nat. Commun.* **10**, 3024 (2019).
50. W. K. Lauenroth, O. E. Sala, Long-term forage production of North American shortgrass steppe. *Ecol. Appl.* **2**, 397–403 (1992).
51. K. J. Anderson-Teixeira *et al*., ForC: A global database of forest carbon stocks and fluxes. *Ecology* **99**, 1507 (2018).
52. M. Zhao, F. A. Heinsch, R. R. Nemani, S. W. Running, Improvements of the MODIS terrestrial gross and net primary production global data set. *Remote Sens. Environ.* **95**, 164–176 (2005).
53. L. Liu *et al*., Broad consistency between satellite and vegetation model estimates of net primary productivity across global and regional scales. *J. Geophys. Res. Biogeosci.* **123**, 3603–3616 (2018).
54. M. A. Friedl *et al*., MODIS Collection 5 global land cover: Algorithm refinements and characterization of new datasets. *Remote Sens. Environ.* **114**, 168–182 (2010).
55. S. D. Prince, J. Haskett, M. Steininger, H. Strand, R. Wright, Net primary production of U.S. Midwest croplands from agricultural harvest yield data. *Ecol. Appl.* **11**, 1194–1205 (2001).
56. Y. Sakamoto, M. Ishiguro, G. Kitagawa, *Akaike Information Criterion Statistics*, (D. Reidel, 1986), Vol. vol. 83, pp. 902–926.
57. R Core Team, *R: A Language and Environment for Statistical Computing*, (R Foundation for Statistical Computing, 2018).
58. J. Pinheiro, D. Bates, S. DebRoy, D. Sarkar, R Core Team, *nlme: Linear and Nonlinear Mixed Effects Models*. R package version 3.1-148, 2020. https://CRAN.R-project.org/package=nlme. Accessed July 10, 2020.